International Conference on Lightning Protection
33rd International Conference on Lightning Protection
25 - 30 September 2016
Estoril, Portugal

The Effect of High Frequency Model of Tower-Footing Grounding Systems on the Back Flashover Rate of Transmission lines

Javad Gholinezhad, Reza shariatinasab
Electrical and Computer Engineering Department
Birjand University
Birjand, Iran,
Shariatinasab@birjand.ac.ir

Keyhan Sheshyekani, Mohammadreza Alemi
Electrical Engineering Department
Shahid Beheshti University
Tehran, Iran
k_sheshyekani@sbu.ac.ir

***Abstract*— This paper presents a probabilistic evaluation, based on Monte-Carlo method, to estimate back flashover rate (BFR) and shielding failure flashover rate (SFFOR) of overhead transmission lines (TLs). In the proposed approach, as opposed to the conventional methods, a wide band model of the tower-footing grounding system is adopted assuming the soil electrical parameters to be either constant or frequency dependent. The statistical parameters affecting the TLs' outage rate are taken into account in the probabilistic studies. Simulations are done for a typical 400-kV transmission line which is modelled in EMTP.RV. From the simulation results, it is found that the BFR of transmission lines is markedly affected by the tower footing grounding system model. This effect is more pronounced when the soil electrical parameters are frequency dependent. It is also found that the SFFOR of the transmission lines is not significantly affected by the wide-band model of the tower-footing grounding system.**

Keywords- Back-flashover; grounding system; shielding failure flashover; wide-band modeling.

I. INTRODUCTION

Lightning is one of the main reasons of insulation breakdown in transmission and distribution lines. This can make the operators and customers incur expenses due to the increase in maintenance services, the need to replacement of damaged equipment and the cut of electricity due to line outages [1]. Generally, surge arresters and shield wires are used for the protection of transmission lines (TLs) against lightning generated overvoltages. These measures are not however enough as there is still a probability of insulation failure following back-flashover (BF) on the regions with high ground resistance. Furthermore, there is a probability of shielding failure (SF) which can result in flashover across the line insulators causing insulation breakdown [2].

So far, extensive studies have been carried on the lightning performance of TLs in order to improve the lightning protection of transmission lines [3]-[7]. However, the previous works have not taken into account the exact wide band model of tower footing-grounding system and use a simple linear or nonlinear resistor [2]-[5] to model the grounding system. Recently, a systematic approach has been presented in [8] and [9] which allows the inclusion of wide band model of grounding systems into the EMTP-like tools. This adequately helps with the exact calculation of lightning generated overvoltages within the electrical networks. With this regard, the effect of wide-band model of grounding system on the lightning performance of a typical transmission line has been evaluated in [9]. However, in [9] the statistical nature of lightning return stroke current parameters has not been taken into account.

Within this context, this papers adopts the same approach presented in [9] for the probabilistic evaluation of lightning performance of a typical transmission line. As a complementary attempt to [9], in this paper, the statistical parameters affecting the TLs' outage rate are taken into account. The BFR and SFFOR of a typical 400 kV transmission line are obtained by establishing a link between Matlab and EMTP.RV. In this study, the tower-footing grounding system is modeled in three different ways namely: 1) static-model, 2) wideband model assuming constant electrical parameters for the soil, and 3) wide-band model assuming frequency-dependent electrical parameters for the soil. The Monte-Carlo method is used for carrying out the required probabilistic studies.

II. LIGHTNING PARAMETERS

The main parameters of the lightning waveform are the peak value (I_p), rise time (t_f) and time to half value (t_h). From the field data on lightning strokes, the probability density function of each lightning parameter is determined by the following equation [10]:

$$p(x) = \frac{1}{\sigma_{\ln x}\sqrt{2\pi}\,x}\exp\left\{-\frac{1}{2}\left(\frac{\ln x - \ln \bar{x}}{\sigma_{\ln x}}\right)^2\right\} \qquad (1)$$

Where σ_{lnx} and $\bar{x}$ are the standard deviation and average of x, respectively. In this paper, Dependence of the peak current magnitude and rise time is considered [10]. The log-normal characteristics of the lightning negative-polarity of first and subsequent return stroke currents are shown in Table I.

TABLE I. STATISTICAL PARAMETERS OF THE LIGHTNING NEGATIVE-POLARITY FIRST STROKE [10]

Parameters	*First stroke*		*Subsequent stroke*	
	Median	σ_{lnx}	Median	σ_{lnx}
I_p (kA)	31.1	0.48	13	0.6447
t_f (μs)	3.83	0.55	0.32	0.6677
t_h (μs)	75	0.58	20	0.69
ρ (I_p, t_f)	0.47			

Having obtained the lightning parameters, a Heidler model can be used to represent the current waveform [11]:

$$i(t) = \frac{I_p}{\eta}\frac{k^n}{1+k^n}e^{-t/\tau_2} \quad (2)$$

where I_p, n and η are the peak current, the current steepness factor and the peak current correction factor, respectively; and $k=t/\tau_1$; τ_1 and τ_2 are time constants that determine the rise time and decay time of the lightning waveform, respectively. First and subsequent current return strokes are shown in Fig.1.

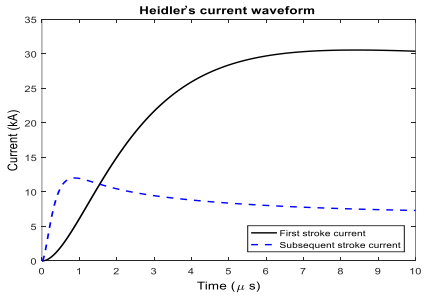

Figure 1. Lightning current waveform

III. TRANSMISSION LINE MODELING

A. Transmission Tower

A multistory model, Fig. 2, is used for transmission tower, where Z_{t1} is the tower top to the upper phase arm, Z_{t2} is the upper to middle, Z_{t3} is the middle to lower, and Z_{t4} is the lower to the tower bottom [12]. The values of the R and L are obtained as follows:

$$R_i = \Delta R_i . h_i, \quad L_i = 2\tau R_i$$

$$\Delta R_1 = \Delta R_2 = \Delta R_3 = \frac{2Z_{t1}}{(h-h_4)}\ln\left(\frac{1}{\alpha_1}\right) \quad (3)$$

$$\Delta R_4 = \frac{2Z_{t4}}{h}\ln\left(\frac{1}{\alpha_4}\right)$$

where h is tower height, $\alpha_1=\alpha_4=0.89$, $c=300$ *m/μs* and the value of 200Ω is considered for surge impedance of all towers.

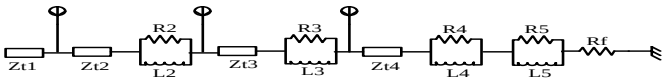

Figure 2. A multistory model of transmission tower.

B. Insulator String

In this paper, the integration method is used for evaluating the effects of non-standard lightning overvoltages. In the integration method, V_0 is the minimum voltage beyond which any breakdown process occurs; and the breakdown time is a function of magnitude and time duration of the applied overvoltage. The integration method is deduced as below [13]:

$$DE = \int_{t_0}^{t} (V(t) - V_0)^k \, dt \quad (4)$$

where DE ($kv^k.\mu s$) is the disruptive effect of the applied impulse voltage, V_0 (kv) is the required minimum voltage, t_0 (μs) is the instant that the instantaneous voltage $V(t)$ exceeds than V_0, k is a factor accounting for the effects of the applied voltage amplitude and time on DE. In this method, breakdown occurs when the integral (DE) becomes equal to or higher than the critical disruptive effect DE^*. Usually, the best possible fit between the computed and experimental voltage-time characteristics under standard lightning impulses determines the appropriate values of DE^* and k. The values of the integration method's parameter are presented in Table II.

TABLE II. INTEGRATION METHOD PARAMETER VALUES IN 400-KV [13]

K=1.36		*K=2.5*	
V_0(kv)	$DE^*(*10^3.kV^{1.36}.\mu s)$	V_0(kv)	$DE^*(*10^6.kV^{2.5}.\mu s)$
1363.0	30.061	849.7	213.579

C. Tower Footing Impedance

In the lightning probabilistic related studies, the grounding impedance is usually modelled by a simple non-linear resistance in which the soil ionization varies with the current magnitude flows through the tower footing [2], [5], [14]-[16]. However, the frequency dependence of soil electrical parameters is ignored [17]-[19]. Note that in the adopted model the range of frequency is supposed to be DC to 2 MHz.

For modeling the frequency dependence of soil electrical parameters, Longmire and Smith proposed the analytical formulae as below [20]:

$$\rho_{\circ}=125\cdot(\frac{p}{10})^{-0.54}(\Omega m)\quad,\quad \varepsilon_{\infty}=5$$

$$\rho(f)=(\rho_{\circ}^{-1}+2\pi\varepsilon_{\circ}\sum_{n=1}^{14}\frac{a_n((\frac{p}{10})^{1.28}\cdot 10^{n-1})(\frac{f}{(\frac{p}{10})^{1.28}\cdot 10^{n-1}})^2}{1+(\frac{f}{(\frac{p}{10})^{1.28}\cdot 10^{n-1}})^2})^{-1} \tag{5}$$

$$\varepsilon_r(f)=\varepsilon_{\infty}+\sum_{n=1}^{14}\frac{a_n}{1+(\frac{f}{(\frac{p}{10})^{1.28}\cdot 10^{n-1}})^2}$$

where f is the frequency ranging from DC to 2 MHz, ρ_0 is the low-frequency resistivity, $\rho(f)$ and $\varepsilon_r(f)$ are the soil resistivity and relative permittivity, respectively and p is the water percentage of soil. In this paper, the grounding system is modeled in three different ways:

1) Static-Model (Conventional):

A simple resistor equals to DC resistance of the grounding system is used to model the grounding system.

2) CP-wide-band:

The wide-band model of the grounding system assuming constant electrical parameters for the soil is used.

3) FD-wide-band:

A wide-band model of the grounding system buried in soil with frequency-dependent electrical parameters is used.

It is noted that in our studies, we assume that no ionization occurs due to the high impulse current injected to the tower-footing grounding system. The wide-band modeling of tower–footing grounding system is explained briefly in the following Section.

IV. Modeling of Grounding System

A. Calculation of the grounding system admittance matrix

To obtain the impedance of the tower-footing grounding system over the desired frequency interval, we use the Method of Moments (MoM) to solve the Electric Field Integral Equation (EFIE) which governs the current distribution along grounding system conductors. The general form of this equation is as follows;

$$t.E^i=\frac{j\omega\mu}{4\pi}\int_i I_i(r')G(r,r')dl \tag{6}$$

where t is the unit vector tangential to wire path l, μ is the magnetic permeability, E^i is the incident electric field by an external source, $G(r,r')$ is the dyadic Green's function for the electric field at r due to a current element at r' and $I_i(r')$ is the unknown induced current along the wire.

By solving the EFIE equation, the current distribution along grounding conductors and hence the electric field within the solution domain is obtained. The voltage rise at the excitation port (or ports) can be then easily obtained as a line integration over the electric field along a pre-specified path. Finally, the values of voltages and currents are used to form the system impedance (or admittance) matrix in the frequency domain as,

$$\mathbf{Y}_g(s)=\mathbf{Z}_g^{-1}(s)=\begin{pmatrix} y_{11}(s) & \cdots & y_{1P}(s)\\ \vdots & \ddots & \vdots\\ y_{P1}(s) & \cdots & y_{PP}(s)\end{pmatrix} \tag{7}$$

where P is the number of ports of the grounding system, $\mathbf{y}_{ij}(s)$ $(i=j)$ represents the self-admittances and $\mathbf{y}_{ij}(s)$ $(i\neq j)$ denotes the mutual admittances between port i and port j. The reader is referred to [9] for further details.

B. Development of the state-space model

The development of the state-space block of the grounding system to be used in EMTP-RV requires the following steps:

1- Pole residue characterization of the admittance matrix: This is done by making use of the matrix pencil method as described in [21] and [22]. In doing so, each vector yij (s) of the admittance matrix Yg(s) can be fitted as,

$$\mathbf{y}_{ij}(s)\approx\{\mathbf{y}_{ij}(s)_{fit}\}=\sum_{m=1}^{M}\frac{R_{m,ij}}{s-a_m}+d_{ij}+se_{ij} \tag{8}$$
$$i=1,2,...,P;\ j=1,2,...,P$$

where a_m and R_m respectively denote the poles and the residues of the system, d and e are optional constant values and M is the number of pre-defined common poles which are the same for each vector. The passivity is enforced to the fitted model to obtain stable time-domain simulations [23].

2- Development of State-Space Model

Once the passive pole-residue model of the grounding system admittance matrix is obtained, one can alternatively formulate it in the form of state-space equations. As the pole-residue model implies a common set of poles for all elements of the admittance matrix $\mathbf{Y}_g(s)$, we have,

$$\mathbf{Y}_g(s)=\sum_{m=1}^{M}\frac{\mathbf{R}_m}{s-a_m}+\mathbf{D}+s\mathbf{E} \tag{9}$$
$$\mathbf{Y}_g(s)=\mathbf{D}+\mathbf{C}(s\mathbf{I}-\mathbf{A})^{-1}\mathbf{B}+s\mathbf{E}$$

where $\mathbf{R}_m$ holds the vector of residues of the elements in the admittance matrix $\mathbf{Y}_g(s)$, M is the order of approximation and $\mathbf{D}$ and $\mathbf{E}$ are the vectors of constant values.

For an P-port grounding system, we assume that the matrices $\mathbf{A}_r$, $\mathbf{B}_r$, and $\mathbf{C}_r$ contain only real poles and their corresponding residues, and $\mathbf{A}_c$, $\mathbf{B}_c$, and $\mathbf{C}_c$ contain only the complex poles and residues, while $\mathbf{A}_c^*$, $\mathbf{B}_c^*$, and $\mathbf{C}_c^*$ hold their corresponding conjugates. After some manipulations (see [24] for further details) the final form of state-space equations reads,

$$\begin{pmatrix}\dot{\tilde{\mathbf{x}}}_1\\ \dot{\tilde{\mathbf{x}}}_2\\ \dot{\tilde{\mathbf{x}}}_3\end{pmatrix}=\begin{bmatrix}\mathbf{A}_r & 0 & 0\\ 0 & \mathrm{Re}(\mathbf{A}_c) & \mathrm{Im}(\mathbf{A}_c)\\ 0 & -\mathrm{Im}(\mathbf{A}_c) & \mathrm{Re}(\mathbf{A}_c)\end{bmatrix}\cdot\begin{pmatrix}\tilde{\mathbf{x}}_1\\ \tilde{\mathbf{x}}_2\\ \tilde{\mathbf{x}}_3\end{pmatrix}+\begin{bmatrix}\mathbf{B}_r\\ 2\,\mathrm{Re}(\mathbf{B}_c)\\ 2\,\mathrm{Im}(\mathbf{B}_c)\end{bmatrix}\cdot\mathbf{v} \tag{10}$$
$$\mathbf{i}=\begin{bmatrix}\mathbf{C}_r & \mathrm{Re}(\mathbf{C}_c) & \mathrm{Im}(\mathbf{C}_c)\end{bmatrix}\cdot\begin{pmatrix}\tilde{\mathbf{x}}_1\\ \tilde{\mathbf{x}}_2\\ \tilde{\mathbf{x}}_3\end{pmatrix}+\mathbf{D}.\mathbf{v}\ .$$

The state-space equations can be directly implemented in EMTP-RV using the state-space block [8].

V. Monte Carlo Method for BFR and SFFOR Analysis

Usually, it is assumed that termination point of lightning surges is distributed uniformly on an impact area [25].

Having an impact area, the Monte Carlo simulation for estimation of BFR and SFFOR can be summarized as follows: 1) generating random values of lightning parameters and coordination of lightning stepped leader *(x, y)* on the impact area, considering their theoretical distribution function; 2) application of an Electro-geometric incidence model (EGM) to determine termination point of impact of each lightning stroke (strokes to tower, phase conductors and ground); 3) evaluating the overvoltage generated by each lightning stroke, depending on the termination point of impact.

Once Monte Carlo simulation was terminated, the lightning flashover rate (LFOR), SFFOR and BFR are determined [3]:

$$SFFOR = N_g .100.d .F_P / N \tag{11}$$

$$BFR = N_g .100.d .F_g / N \tag{12}$$

$$LFOR = BFR + SFFOR \tag{13}$$

where N is number of runs, N_g=*1* (*flashes/km^2.year*) is the ground flash density, F_p and F_g are the number of flashovers caused by strokes to phase conductor and shield wire, respectively; d is the maximum width of impact area that corresponds to the maximum peak current magnitude generated by the Monte Carlo simulation.

VI. Case Study

The proposed approached is used for the study of a 400 kV overhead line with an insulation level of 1450 kV. The typical line configuration is shown in Fig. 3 and the line specifications are presented in Table III.

TABLE III. Line conductor characteristic

	Type	Diameter (cm)	Resistance Ω/km
Phase conductors	CURLEW	3.163	0.05501
Shield wire	94S	1.26	0.642

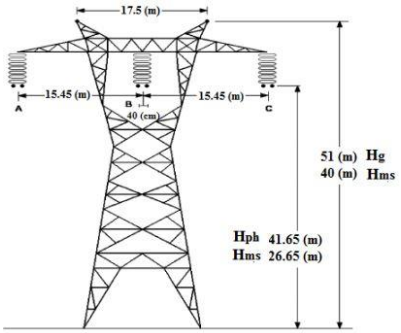

Figure 3. Tower configuration (values in brackets are midspan heights)

The towers are represented by multi-story model, whose parameters can be calculated as described in Section III. The transmission line is modelled by five spans of 450 *m* length which modeled by multi-phase untransposed frequency-dependent distributed parameter, i.e. J. Marti's model [26]. To avoid reflection from the ending far, the line is terminated to a 40 km additional section. The representation of insulator strings is based on the integrated model of Section III. The procedure involves the calculation of the grounding system admittance matrix and the representation of its state-space model to be incorporated in the EMTP.RV.

Having obtained different parameters of lightning surge and initial point of lightning occurrence on the struck area, the EGM model of transmission line [27] was constructed in order to determine the termination point of impact of each lightning stroke (ground, phase conductor and tower). The aforementioned steps are performed in MATLAB environment. Once the termination point of impact of each stroke has been determined, the resultant EMTP simulations are performed to estimate the related overvoltages. The lightning related studies by Monte Carlo simulation are then carried out.

VII. Simulation Results

To obtain the distribution function of lightning parameters, the random values of each parameter is generated. Convergence of Monte Carlo method is checked by comparing density function of the randomly generated variables to their theoretical functions. A 5% of error is set for this propose. In this paper, the convergence was occurred after 30000 runs. As an example, Fig. 4 presents the distribution of generated values of current magnitude and rise time with the correlation between them.

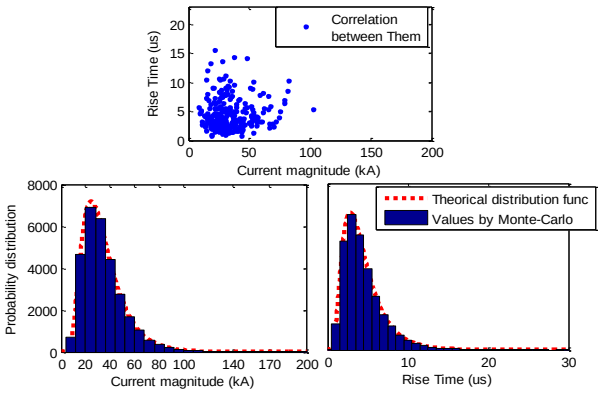

Figure 4. Distribution of randomly generated values of lightning current amplitude and front time with their statistical correlation.

The grounding system of each tower is modeled using the state-space block. The analyses are done for two cases of tower-footing grounding system structure; a one-port vertical rod and a four-port simple square grid [28].

We first study the transmission line with a rod-shaped tower-footing grounding system. The grounding rod has a length of 15m and a cross section radius of 12.5mm. The analysis is done for four different soil resistivities; ρ=50 Ωm, ρ=100 Ωm, ρ =500 Ωm and ρ =1000 Ωm all having the same relative permittivity of ε_r=20. These values of resistivities are used in (5) as ρ_0 for the case of frequency dependent soil parameters.

To produce state-space block of the grounding system which is compatible with EMTP.RV, the pole-residue model generated by MPM is obtained for all cases.

Fig. 5 shows the amplitude of the harmonic impedance of the vertical grounding electrode, computed using the MoM approach presented in Section IV. The impedance is calculated in frequency range of DC to 2 MHz for both soils with constant and frequency-dependent electrical parameters.

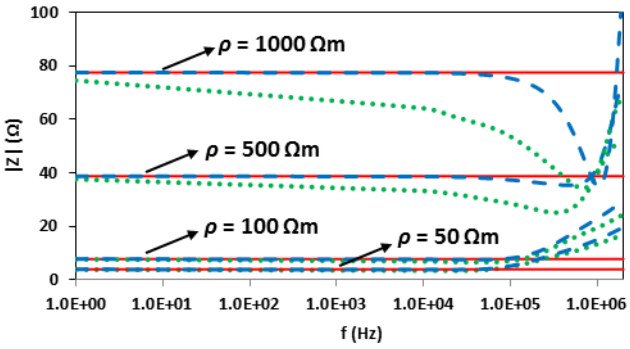

Figure 5. Self-impedances of the vertical rod for different soil resistivities. Red-solid line: simple resistor equal to the dc resistance, blue-dashed line: soil with constant electrical parameters, green-dotted line: soil with frequency-dependent electrical parameters. Adapted from [9].

Fig. 6 shows the overvoltages across the insulator string caused by lightning strokes to shield wire, for different types of grounding system modelling.

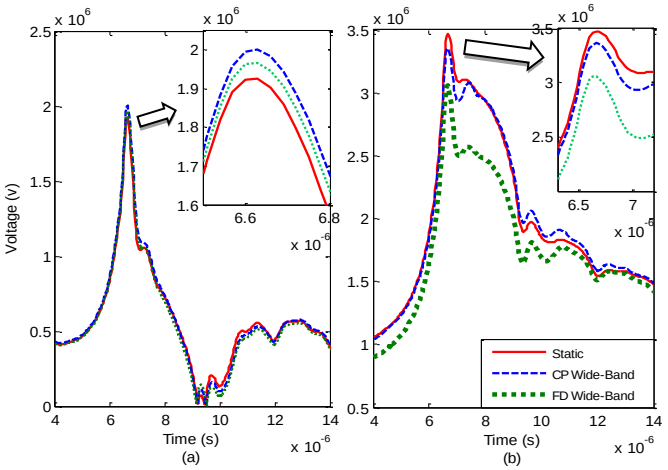

Figure 6. Overvoltages across insulator string in Rod-shape grounding system. Return stroke (100 kA/3.83 μs/75 μs) (a) ρ=100 Ω.m, (b) ρ=1000 Ω.m.

The results show that the estimated values of the overvoltages across the insulator string are markedly affected by the adopted grounding system model. As it is seen, the effect of wide band modeling of grounding system is more pronounced when the soil electrical parameters are considered to be frequency dependent. Also seen that the effect of wide band model of grounding system is more significant for the soils with high resistivities. From the reported results, it can be seen that for the soil with low resistivity, i.e. ρ=100 Ωm, the calculated overvoltages associated with the CP Wide-band model are higher than the case of FD Wide-band and Static models. For this case, the difference between the max and min values of the overvoltage waveshape is about 100 kv. However, for the soil with high resistivity, ρ=1000 Ω.m, the maximum value of generated overvoltages across the insulator string belongs to the static model and the difference between the min and max values of the overvoltage waveshape increases to 500 kV.

The LFOR of transmission line as a function of the soil resistivity for different models of grounding impedance is presented in Table IV and Table V, for Rod-shape and grid-shape of grounding system, respectively. All results were deduced after 30000 runs.

TABLE IV. OUTAGE RATES OF TRANSMISSION LINE FOR DIFFERENT MODELLING OF ROD-SHAPE GROUNDING SYSTEM

Soil resistivity	**Grounding system models**	*First Stroke*			*Subsequent Stroke*		
		BFR	*SFFOR*	*LFOR*	*BFR*	*SFFOR*	*LFOR*
ρ=100	ST	3.861	1.898	5.760	0.516	1.109	1.62
	CP	4.181	1.898	6.080	0.700	1.109	1.80
	FD	4.142	1.898	6.041	0.678	1.109	1.78
ρ=500	ST	7.381	1.894	9.275	1.275	1.088	2.36
	CP	7.496	1.894	9.390	1.322	1.088	2.41
	FD	7.168	1.894	9.062	1.211	1.088	2.29
ρ=1000	ST	9.518	1.885	11.40	1.911	1.060	2.97
	CP	9.147	1.885	11.03	1.740	1.060	2.80
	FD	8.465	1.890	10.35	1.635	1.065	2.70

TABLE V. OUTAGE RATES OF TRANSMISSION LINE FOR DIFFERENT MODELLING OF GRID-SHAPE GROUNDING SYSTEM

Soil resistivity	Grounding system models	First Stroke			Subsequent Stroke		
		BFR	*SFFOR*	*LFOR*	*BFR*	*SFFOR*	*LFOR*
ρ=100	ST	3.673	1.898	5.572	0.485	1.109	1.59
	CP	3.980	1.847	5.828	0.690	1.109	1.79
	FD	3.938	1.898	5.836	0.658	1.109	1.76
ρ=500	ST	6.950	1.894	8.844	1.234	1.088	2.32
	CP	7.027	1.894	8.921	1.272	1.088	2.36
	FD	6.830	1.894	8.752	1.187	1.088	2.27
ρ=1000	ST	8.964	1.890	10.85	1.860	1.064	2.92
	CP	8.599	1.892	10.49	1.662	1.064	2.72
	FD	7.812	1.894	9.706	1.568	1.070	2.63

According to the results presented in these tables, the wide-band modeling of grounding system, can remarkably affect the *BFR* and *SFFOR* compared to the static model. It should be mentioned that the soils with low resistivity (ρ=100 Ω.m) has an inductive behavior; then, in this case, *BFR* for wide-band model is higher than the static model. However, the difference between *BFR* calculated by wide-band and static modeling of grounding system is increased as soil resistivity increases. Also, because of the capacitive behavior of the soil with a high resistivity (ρ=1000 Ω.m), *BFR* in the case of wide-band modeling is lower than *BFR* for static model.

It is also seen from the reported results that the modeling type of the grounding system does not significantly influence the estimated *SFFOR*. In the case of subsequent strokes, similar to the first strokes, the wide band modeling of tower-footing grounding system, in particular for highly resistive soils, decreases the probability of *LFOR* compared to the case of soil with constant electrical parameters.

VIII. CONCLUSION

A probabilistic procedure based on Monte Carlo simulation has been carried out for the calculation of lightning performance of transmission lines considering wide band model for the tower-footing grounding system.

In the Monte Carlo procedure, random lightning parameters and termination point of impact of each lightning stroke (phase conductors, shield wires, or ground) were first calculated. Thereafter, the generated overvoltage by each stroke is calculated by simulations performed by EMTP.RV. The procedure was continued until the convergence of the Monte Carlo simulation was achieved.

From the results, it was found that the wide-band model of tower-footing grounding system can affect (either decrease or increase) the generated overvoltages and the resultant value of the peak magnitude across the insulator string of transmission lines. This effect is determined by the soil electrical parameters. Moreover, the frequency dependence of soil electrical parameters generally increases *BFR* for the soils with low resistivity compared to the case of soil with constant electrical parameters. The variation of *BFR* is quite the opposite for the soils with high resistivity, so that the estimated value of *BFR* reduces for the frequency dependence modelling of soil compared to its static model. However, the modeling of the grounding system does not significantly influence *SFFOR*.

REFERENCES

[1] A. R. Hileman, Insulation coordination for power systems. New York, NY, USA: Marcel Dekker, 1999.

[2] R. Shariatinasab, J. G. Safar, and H. Falaghi, "Optimisation of arrester location in risk assessment in distribution network," Generation, Transmission & Distribution, IET, vol. 8, no. 1, pp. 151-159, 2014.

[3] J. A. Martinez, F. C. Aranda, "Lightning performance analysis of overhead transmission lines using the EMTP," IEEE Trans. Power Del., vol. 20, no. 3, pp. 2200-2210, 2005.

[4] M. A. Araújo, and et al, "Practical methodology for modeling and simulation of a lightning protection system using metal-oxide surge arresters for distribution lines," Electric Power Systems Research, vol. 118, pp. 47-54, 2015.

[5] R. Shariatinasab, B. Vahidi, and S. H. Hosseinian, "Statistical evaluation of lightning-related failures for the optimal location of surge arresters on the power networks," IET generation, transmission & distribution, vol. 3, no. 2, pp. 129-144, 2009.

[6] M. S. Banjanin, M. S. Savić, and Z. M. Stojković, "Lightning protection of overhead transmission lines using external ground wires," Electric Power Systems Research, vol. 127, pp. 206-212, 2015.

[7] F. Mahmood, A. S. Nehmdoh, and M. Lehtonen, "Effect of combined AC and lightning-induced overvoltages on the risk of MV insulator flashovers above lossy ground," Electric Power Systems Research, vol. 127, pp. 101-108, 2015.

[8] K. Sheshyekani, M. Akbari, B. Tabei, and R. Kazemi, "Wide-band modeling of large grounding systems to interface with electromagnetic transient solvers," IEEE Trans. Power Del., vol. 29, no. 4, pp. 1868–1876, Aug. 2014.

[9] M. R. Alemi, and K. Sheshyekani, "Wide-Band Modeling of Tower-Footing Grounding Systems for the Evaluation of Lightning Performance of Transmission Lines," IEEE Trans. Electromagn. Compat, vol. 57, no. 6, pp. 1627-1636, July 2015.

[10] P. Chowdhuri, and et al, "Parameters of lightning strokes: a review," IEEE Trans. Power Del., vol. 20, no. 1, pp. 346-358, 2005.

[11] F. Heidler, J. M. Cvetic, and B. V. Stanic, "Calculation of lightning current parameters," IEEE Trans. Power Del., vol. 14, no. 2, pp. 399–404, Apr. 1999.

[12] M. Ishii, T. Kawamura, T. Kouno, E. Ohsaki, K. Shiokawa, K. Murotani, and T. Higuchi, "Multistory transmission tower model for lightning surge analysis," IEEE Trans. Power Del., vol. 6, no. 3, pp. 1327-1335, 1991.

[13] Z. G. Datsios, P. N. Mikropoulos, and T. E. Tsovilis, "Estimation of the minimum shielding failure flashover current for first and subsequent lightning strokes to overhead transmission lines," Electric Power Systems Research, vol. 113, pp. 141-150, 2014.

[14] J. A. Martinez, F. C. Aranda, "Tower Modeling for Lightning Analysis of Overhead Transmission Lines", IEEE Trans on Power Delivery, Vol. 2, pp. 1212-1217, June 2005.

[15] P. Sarajcev, "Monte Carlo method for estimating backflashover rates on high voltage transmission lines," Electric Power Systems Research, vol. 119, pp. 247-257, 2015.

[16] R. Shariatinasab, J. G. Safar, and M.A. Mobarakeh, "Development of an adaptive neural-fuzzy inference system based meta-model for estimating lightning related failures in polluted environments," Science, Measurement & Technology, IET, vol. 8, no. 4, pp.187-195, 2014.

[17] M. Akbari, K. Sheshyekani, A. Pirayesh, F. Rachidi, M. Paolone, A. Borghetti, and C.A. Nucci, "Evaluation of Lightning Electromagnetic Fields and Their Induced Voltages on Overhead Lines Considering the Frequency-Dependence of Soil Electrical Parameters," IEEE Trans. Electromagn. Compat., vol. 55, no. 6, pp. 1210-1219, Dec. 2013.

[18] K. Sheshyekani, and M. Akbari, "Evaluation of Lightning-Induced Voltages on Multi-conductor Overhead Lines Located Above a Lossy

Dispersive Ground," IEEE Trans. Power Del., vol. 29, no. 2, pp. 683-690, 2014.

[19] M. Akbari, K. Sheshyekani, and M. R. Alemi "The effect of frequency dependence of soil electrical parameters on the lightning performance of grounding systems," IEEE Trans. Electromagn. Compat., vol. 55, no. 4, pp. 739-746, Aug. 2013.

[20] C. L. Longmire and K. S. Smith, "A universal impedance for soils," Mission Research Corp., Santa Barbara, CA, Rep. DNA3788T, Oct. 1975.

[21] K. Sheshyekani, H. R. Karami, P. Dehkhoda, M. Paolone, and F. Rachidi, "Application of the Matrix Pencil Method to Rational Fitting of Frequency-Domain Responses," IEEE Trans Power Del., vol. 27, no. 4, pp. 2399 - 2408, Oct. 2012.

[22] K. Sheshyekani, and B. Tabei, "Multiport frequency-dependent network equivalent using a modified matrix pencil method", IEEE Trans. Power Del., vol. 23, no. 5, pp. 2340-2348, Oct. 2014.

[23] B. Gustavsen, "Fast passivity enforcement for pole-residue models by perturbation of residue matrix eigenvalues," IEEE Trans. Power Del., vol. 23, no. 4, pp. 2278-2285, Oct. 2008.

[24] B. Gustavsen, and H. M. J. De Silva, "Inclusion of rational models in an electromagnetic transients program: Y-parameters, Z-parameters, S-parameters, transfer functions", IEEE Trans. Power Del., vol. 28, no. 2, pp. 1164-1174, April 2013.

[25] E. Bullich-Massague, and et al, "Optimization of surge arrester locations in overhead distribution networks," IEEE Trans. Power Del., vol. 30, no. 2, pp.647-683, 2015.

[26] J. R. Marti, "Accurate modeling of frequency-dependent transmission lines in electromagnetic transient simulations," IEEE Trans. Power Appl. Syst., vol. PAS-101, no. 1, pp. 147–157, 1982.

[27] IEEE Std. 1243, "IEEE Guide for Improving the Lightning Performance of Transmission Lines", 1997.

[28] L. Grcev, and M. Popov, "On high-frequency circuit equivalents of a vertical ground rod," IEEE Trans. Power Del., vol. 20, no. 2, pp. 1598-1603, April 2005.